Journal of Engineering Mathematics **26**: 415–428, 1992.

The initial boundary-layer flow past a translating and spinning rotational symmetric body

MEHMET CEM ECE

Trakya University, Mechanical Engineering Department, Edirne, Turkey

Received 23 July 1991; accepted in revised form 25 November 1991

Abstract. The boundary-layer flow on an impulsively started translating and spinning rotational symmetric body is considered. The stream function and the swirl component of the velocity are expanded in series in powers of time. Leading and first order solutions are obtained analytically and the second order solutions are determined numerically. The results are applied to a translating and spinning sphere and the rotation is found to reduce the friction drag and facilitate flow separation.

1. Introduction

Three-dimensional boundary-layer flows have a variety of applications in engineering such as swept wing, corner fairings and spinning projectiles. The absence of known three-dimensional potential-flow solutions prevents the three-dimensional boundary-layer analysis in most cases. Three-dimensional boundary-layer separation also shows significant differences from that of the two-dimensional case.

A rotational symmetric body presents a preliminary case for general three-dimensional boundary layers. An axisymmetric boundary-layer flow over a rotational symmetric body set into axial motion impulsively was first investigated by Boltze [1]. Boltze expanded the stream function in series in powers of time and obtained numerical solutions for the terms in powers up to and including t^3. Dennis and Walker [2] improved the accuracy of the Boltze solution for the boundary-layer flow over an impulsively started sphere and obtained numerical solutions up to and including terms of $O(t^7)$. Dennis and Walker [3] also carried out numerical solutions of the unsteady flow past an impulsively started sphere for both finite Reynolds numbers and the boundary-layer case, and extended the results to larger values of time.

The flow is further complicated in the case of moving walls. The number of solutions to three-dimensional boundary-layer flows including the swirl component of velocity are very few. Flow about a spinning body of revolution was investigated by Illingworth [4], Chu and Tifford [5], Schlichting [6] and Hoskin [7]. These are all momentum-integral approximations and of uncertain accuracy. The boundary-layer flow on a rotating sphere in a fluid at rest shows different characteristics near the poles and near the equator as discussed by Howarth [8], Sawatzki [9] and Dumarque et al. [10]. Measurements of Luthander and Rydberg [11] and the study of Hoskin [7] show that there is a marked influence of rotation on drag and separation on a spinning sphere in an axial stream.

The unsteady boundary-layer flow past an impulsively started translating and spinning rotational symmetric body of general shape is considered in the present paper. Initial stages of the phenomenon is investigated by expanding the stream function and the swirl velocity in series in powers of time. The effects of the body shape and the rotation rate are identified. Solutions up to and including terms of $O(t)$ are obtained analytically. The terms of $O(t^2)$ are determined numerically. The results are applied to a translating and spinning sphere.

2. Basic equations

Curvilinear coordinates (x^*, y^*, Θ) are used in the formulation of the problem. Geometry and the coordinate system are illustrated in Fig. 1. Here x^* is the dimensional coordinate measured parallel to the surface from the nose of the body, y^* is dimensional normal coordinate to the surface and Θ is the circumferential angle. The dimensional local surface radius measured from the symmetry axis is denoted by $r^*(x^*)$. The body is assumed to be set into motion impulsively with a constant axial velocity U_0 and angular velocity Ω. Let u^*, v^* and w^* be the dimensional velocity components in the x^*, y^* and Θ directions respectively and t^* be the dimensional time measured from the impulsive start.

Dimensionless variables used in the analysis are defined as

$$x = \frac{x^*}{L}, \quad y = \frac{y^*}{L}, \quad r = \frac{r^*}{L}, \quad t = \frac{U_0 t^*}{L}, \tag{2.1}$$

$$u = \frac{u^*}{U_0}, \quad v = \frac{v^*}{U_0}, \quad w = \frac{w^*}{U_0}, \quad \omega = \frac{\Omega L}{U_0}, \tag{2.2}$$

where L is the characteristic length of the motion.

The boundary-layer equations given by Mangler [12] are the continuity

$$\frac{\partial(ru)}{\partial x} + \frac{\partial(rv)}{\partial y} = 0, \tag{2.3}$$

x momentum

$$\frac{\partial u}{\partial t} + u\frac{\partial u}{\partial x} + v\frac{\partial u}{\partial y} - \frac{w^2}{r}\frac{\mathrm{d}r}{\mathrm{d}x} = U_e\frac{\mathrm{d}U_e}{\mathrm{d}x} + \frac{1}{\mathrm{Re}}\frac{\partial^2 u}{\partial y^2}, \tag{2.4}$$

and Θ momentum

$$\frac{\partial w}{\partial t} + u\frac{\partial w}{\partial x} + v\frac{\partial w}{\partial y} + \frac{uw}{r}\frac{\mathrm{d}r}{\mathrm{d}x} = \frac{1}{\mathrm{Re}}\frac{\partial^2 w}{\partial y^2}, \tag{2.5}$$

where U_e is the axial boundary layer edge velocity and $\mathrm{Re} = U_0 L/\nu$ is the Reynolds number, ν being the kinematic viscosity of the fluid. Boundary conditions to be satisfied are

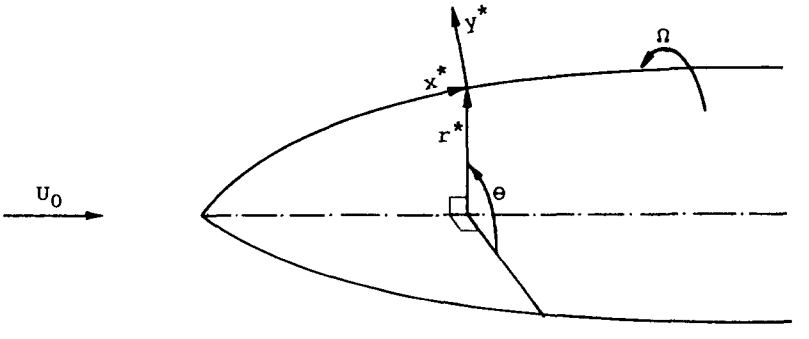

Fig. 1. Geometry and the coordinate system.

$$u(x,0,t)=0\,,\qquad v(x,0,t)=0\,,\qquad w(x,0,t)=\omega r\,, \tag{2.6}$$

$$\lim_{y\to\infty} u(x,y,t)=0\,,\qquad \lim_{y\to\infty} w(x,y,t)=0\,. \tag{2.7}$$

A stream function is defined according to

$$ru=\frac{\partial\psi}{\partial y}\,,\qquad rv=-\frac{\partial\psi}{\partial x}\,. \tag{2.8}$$

Boundary layer variables used by Ece et al. [13] are adapted and given by

$$y=Kn\,,\qquad \psi=K\Psi\,,\qquad K=2\sqrt{t/\mathrm{Re}}\,. \tag{2.9}$$

This transformation magnifies the thin boundary layer and removes the initial singularity associated with the impulsive start of the motion. The functions $F(x,n,t)$ and $G(x,n,t)$ are defined as follows:

$$\Psi=rU_eF\,,\qquad w=\omega rG\,. \tag{2.10}$$

It may be shown that

$$u=U_e\frac{\partial F}{\partial n}\,,\qquad v=-K\left[\left(\frac{1}{r}\frac{\mathrm{d}r}{\mathrm{d}x}U_e+\frac{\mathrm{d}U_e}{\mathrm{d}x}\right)F+U_e\frac{\partial F}{\partial x}\right]. \tag{2.11}$$

The continuity is satisfied and the momentum equations are written as

$$\frac{\partial^3F}{\partial n^3}+2n\frac{\partial^2F}{\partial n^2}=4t\left\{\frac{\partial^2F}{\partial t\,\partial n}-\omega^2\frac{rr'}{U_e}G^2-U_e'+\frac{\partial F}{\partial n}\left(U_e'\frac{\partial F}{\partial n}+U_e\frac{\partial^2F}{\partial x\,\partial n}\right)\right.$$
$$\left.-\frac{\partial^2F}{\partial n^2}\left[\left(\frac{r'}{r}U_e+U_e'\right)F+U_e\frac{\partial F}{\partial x}\right]\right\}, \tag{2.12}$$

$$\frac{\partial^2G}{\partial n^2}+2n\frac{\partial G}{\partial n}=4t\left\{\frac{\partial G}{\partial t}+U_e\frac{\partial F}{\partial n}\left(2\frac{r'}{r}G+\frac{\partial G}{\partial x}\right)-\frac{\partial G}{\partial n}\left[\left(\frac{r'}{r}U_e+U_e'\right)F+U_e\frac{\partial F}{\partial x}\right]\right\}. \tag{2.13}$$

The boundary conditions reduce to

$$F(x,0,t)=0\,,\qquad \left.\frac{\partial F}{\partial n}\right|_{n=0}=0\,,\qquad G(x,0,t)=1\,, \tag{2.14}$$

$$\lim_{n\to\infty}\frac{\partial F}{\partial n}=1\,,\qquad \lim_{n\to\infty}G(x,n,t)=0\,. \tag{2.15}$$

3. Time series solution

The initial stages of the motion may be investigated by expanding the functions $F(x,n,t)$ and $G(x,n,t)$ in powers of time as

$$F(x,n,t)=F_0(n)+tF_1(x,n)+t^2F_2(x,n)+\cdots\,, \tag{3.1}$$

$$G(x, n, t) = G_0(n) + tG_1(x, n) + t^2 G_2(x, n) + \cdots . \tag{3.2}$$

Substitution of Eqs (3.1) and (3.2) into Eqs (2.12) and (2.13) yields the leading order equations as

$$F_0''' + 2nF_0'' = 0 , \tag{3.3}$$

$$G_0'' + 2nG_0' = 0 , \tag{3.4}$$

with the boundary conditions

$$F_0(0) = 0 , \qquad F_0'(0) = 0 , \qquad G_0(0) = 1 , \tag{3.5}$$

$$\lim_{n\to\infty} F_0'(n) = 1 , \qquad \lim_{n\to\infty} G_0(n) = 0 . \tag{3.6}$$

Solutions of Eqs (3.3) and (3.4) satisfying the boundary conditions (3.5) and (3.6) are

$$F_0(n) = n \operatorname{erf}(n) + \frac{1}{\sqrt{\pi}} (e^{-n^2} - 1) , \tag{3.7}$$

$$G_0(n) = 1 - \operatorname{erf}(n) . \tag{3.8}$$

The $O(t)$ terms define the first order equations and the form of the momentum equations suggests that the functions $F_1(x, n)$ and $G_1(x, n)$ must be of the form

$$F_1(x, n) = U_e' F_{11}(n) + \frac{r'}{r} U_e F_{12}(n) + \omega^2 \frac{rr'}{U_e} F_{13}(n) , \tag{3.9}$$

$$G_1(x, n) = U_e' G_{11}(n) + \frac{r'}{r} U_e G_{12}(n) . \tag{3.10}$$

The functions $F_{1i}(n)$ $(i = 1, 2, 3)$ and $G_{1j}(n)$ $(j = 1, 2)$ satisfy the following ordinary differential equations

$$F_{11}''' + 2nF_{11}'' - 4F_{11}' = 4(F_0'^2 - F_0F_0'' - 1) , \tag{3.11}$$

$$F_{12}''' + 2nF_{12}'' - 4F_{12}' = -4F_0F_0'' , \tag{3.12}$$

$$F_{13}''' + 2nF_{13}'' - 4F_{13}' = -4G_0^2 , \tag{3.13}$$

$$G_{11}'' + 2nG_{11}' - 4G_{11} = -4F_0G_0' , \tag{3.14}$$

$$G_{12}'' + 2nG_{12}' - 4G_{12} = 4(2F_0'G_0 - F_0G_0') , \tag{3.15}$$

and are subject to the boundary conditions

$$F_{1i}(0) = 0 , \qquad F_{1i}'(0) = 0 , \qquad \lim_{n\to\infty} F_{1i}'(n) = 0 ; \quad i = 1, 2, 3 , \tag{3.16}$$

$$G_{1j}(0) = 0 , \qquad \lim_{n\to\infty} G_{1j}(n) = 0 ; \quad j = 1, 2 . \tag{3.17}$$

Solutions of these equations are

$$F_{11}(n) = -\left(\frac{8}{3\pi} + 3\right) p(n) - q(n) + \frac{2}{3}\, r(n) + n - \frac{11}{6\sqrt{\pi}}\, \mathrm{e}^{-n^2}\, \mathrm{erf}(n) - \frac{1}{2}\, n\, \mathrm{erf}^2(n) - \frac{2}{3\sqrt{\pi}}\, \mathrm{erf}(n) + \frac{8}{3\sqrt{2\pi}}\, \mathrm{erf}(\sqrt{2}n)\,, \tag{3.18}$$

$$F_{12}(n) = \left(\frac{16}{3\pi} - 1\right) p(n) + q(n) - \frac{2}{3}\, r(n) - \frac{7}{6\sqrt{\pi}}\, \mathrm{e}^{-n^2}\, \mathrm{erf}(n) - \frac{1}{2}\, n\, \mathrm{erf}^2(n) - \frac{2}{3\sqrt{\pi}}\, \mathrm{erf}(n) + \frac{4}{3\sqrt{2\pi}}\, \mathrm{erf}(\sqrt{2}n)\,, \tag{3.19}$$

$$F_{13}(n) = \left(\frac{8}{\pi} - 6\right) p(n) + 2q(n) - \frac{4}{3}\, r(n) + n - 2\left[n\, \mathrm{erf}(n) + \frac{1}{\sqrt{\pi}}\, (\mathrm{e}^{-n^2} - 1)\right] + \frac{2}{3\sqrt{\pi}}\, \mathrm{e}^{-n^2}\, \mathrm{erf}(n) - \frac{4}{3\sqrt{2\pi}}\, \mathrm{erf}(\sqrt{2}n)\,, \tag{3.20}$$

$$G_{11}(n) = \left(1 - \frac{16}{3\pi}\right) f(n) - g(n) + \frac{1}{\sqrt{\pi}}\, n\, \mathrm{e}^{-n^2}\, \mathrm{erf}(n) + \left(\frac{1}{2} + n^2\right) \mathrm{erf}^2(n) + \frac{4}{3\pi}\, \mathrm{e}^{-n^2}\,, \tag{3.21}$$

$$G_{12}(n) = \left(\frac{32}{3\pi} - 3\right) f(n) + 3g(n) - \frac{7}{\sqrt{\pi}}\, n\, \mathrm{e}^{-n^2}\, \mathrm{erf}(n) - 2\, \mathrm{erf}(n) + \left(\frac{1}{2} - 3n^2\right) \mathrm{erf}^2(n) - \frac{4}{\pi}\, \mathrm{e}^{-2n^2} + \frac{4}{3\pi}\, \mathrm{e}^{-n^2}\,, \tag{3.22}$$

where

$$p(n) = \frac{1}{6}\, n^3 - \frac{1}{6}\left[n^3\, \mathrm{erf}(n) + \frac{1}{\sqrt{\pi}}\, (n^2 + 1)\, \mathrm{e}^{-n^2} - \frac{1}{\sqrt{\pi}}\right] + \frac{1}{4}\, n(1 - \mathrm{erf}(n))\,, \tag{3.23}$$

$$q(n) = \frac{1}{6}\, n^3 + \frac{1}{6}\left[n^3\, \mathrm{erf}(n) + \frac{1}{\sqrt{\pi}}\, (n^2 + 1)\, \mathrm{e}^{-n^2} - \frac{1}{\sqrt{\pi}}\right] + \frac{1}{4}\, n(1 + \mathrm{erf}(n))\,, \tag{3.24}$$

$$r(n) = \frac{1}{2}\, n^3\, \mathrm{erf}^2(n) + \frac{1}{\sqrt{\pi}}\, n^2\, \mathrm{e}^{-n^2}\, \mathrm{erf}(n) + \frac{1}{2\pi}\, n\, \mathrm{e}^{-2n^2}\,, \tag{3.25}$$

$$f(n) = \frac{1}{2}\, n\left(n - n\, \mathrm{erf}(n) - \frac{1}{\sqrt{\pi}}\, \mathrm{e}^{-n^2}\right) + \frac{1}{4}\, (1 - \mathrm{erf}(n))\,, \tag{3.26}$$

$$g(n) = \frac{1}{2}\, n\left(n + n\, \mathrm{erf}(n) + \frac{1}{\sqrt{\pi}}\, \mathrm{e}^{-n^2}\right) + \frac{1}{4}\, (1 + \mathrm{erf}(n))\,. \tag{3.27}$$

Balancing the $O(t^2)$ terms in Eqs (2.12) and (2.13) determines the second order equations. The form of these equations suggests that the functions $F_2(x, n)$ and $G_2(x, n)$ must be of the form

$$F_2(x, n) = U_e'^2 F_{21}(n) + U_e U_e'' F_{22}(n) + U_e U_e' \frac{r'}{r}\, F_{23}(n) + \left(\frac{r' U_e}{r}\right)^2 F_{24}(n) + \frac{r''}{r}\, U_e^2 F_{25}(n) + \omega^2\left[r'^2 F_{26}(n) + r r'' F_{27}(n) + \frac{r r' U_e'}{U_e}\, F_{28}(n)\right], \tag{3.28}$$

$$G_2(x,n) = U_e'^2 G_{21}(n) + U_e U_e'' G_{22}(n) + U_e U_e' \frac{r'}{r} G_{23}(n) + \left(\frac{r' U_e}{r}\right)^2 G_{24}(n) + \frac{r''}{r} U_e^2 G_{25}(n) + \omega^2 \left[r'^2 G_{26}(n) + r r'' G_{27}(n) \right]. \tag{3.29}$$

The functions $F_{2i}(n)$ $(i = 1-8)$ and $G_{2j}(n)$ $(j = 1-7)$ satisfy the following ordinary differential equations

$$F_{21}''' + 2nF_{21}'' - 8F_{21}' = 4(2F_0'F_{11}' - F_0''F_{11} - F_0F_{11}''), \tag{3.30}$$

$$F_{22}''' + 2nF_{22}'' - 8F_{22}' = 4(F_0'F_{11}' - F_0''F_{11}), \tag{3.31}$$

$$F_{23}''' + 2nF_{23}'' - 8F_{23}' = 4(3F_0'F_{12}' - F_0''F_{11} - 2F_0''F_{12} - F_0F_{11}'' - F_0F_{12}''), \tag{3.32}$$

$$F_{24}''' + 2nF_{24}'' - 8F_{24}' = 4(-F_0'F_{12}' - F_0F_{12}''), \tag{3.33}$$

$$F_{25}''' + 2nF_{25}'' - 8F_{25}' = 4(F_0'F_{12}' - F_0''F_{12}), \tag{3.34}$$

$$F_{26}''' + 2nF_{26}'' - 8F_{26}' = 4(-2G_0G_{12} - 2F_0''F_{13} + F_0'F_{13}' - F_0F_{13}''), \tag{3.35}$$

$$F_{27}''' + 2nF_{27}'' - 8F_{27}' = 4(F_0'F_{13}' - F_0''F_{13}), \tag{3.36}$$

$$F_{28}''' + 2nF_{28}'' - 8F_{28}' = 4(-2G_0G_{11} + F_0'F_{13}' - F_0F_{13}''), \tag{3.37}$$

$$G_{21}'' + 2nG_{21}' - 8G_{21} = 4(-G_0'F_{11} - F_0G_{11}'), \tag{3.38}$$

$$G_{22}'' + 2nG_{22}' - 8G_{22} = 4(F_0'G_{11} - G_0'F_{11}), \tag{3.39}$$

$$G_{23}'' + 2nG_{23}' - 8G_{23} = 4(2F_0'G_{11} + F_0'G_{12} + 2G_0F_{11}' - G_0'F_{11} - 2G_0'F_{12} - F_0G_{11}' - F_0G_{12}'), \tag{3.40}$$

$$G_{24}'' + 2nG_{24}' - 8G_{24} = 4(F_0'G_{12} + 2G_0F_{12}' - F_0G_{12}'), \tag{3.41}$$

$$G_{25}'' + 2nG_{25}' - 8G_{25} = 4(F_0'G_{12} - G_0'F_{12}), \tag{3.42}$$

$$G_{26}'' + 2nG_{26}' - 8G_{26} = 4(2G_0F_{13}' - 2G_0'F_{13}), \tag{3.43}$$

$$G_{27}'' + 2nG_{27}' - 8G_{27} = -4G_0'F_{13}, \tag{3.44}$$

and are subject to the boundary conditions

$$F_{2i}(0) = 0, \qquad F_{2i}'(0) = 0, \qquad \lim_{n\to\infty} F_{2i}'(n) = 0; \quad i = 1-8, \tag{3.45}$$

$$G_{2j}(0) = 0, \qquad \lim_{n\to\infty} G_{2j}(n) = 0; \quad j = 1-7. \tag{3.46}$$

The complexity of the right hand sides of the governing equations increases very rapidly. Equations (3.30)–(3.44) were solved numerically using the Thomas algorithm. The numeri-

cal mesh size was taken to be $h = 0.01$ to ensure a good accuracy. The boundary conditions at infinity were approximately satisfied at $n = 6$ and later verified by examining the solution.

4. Results

The time series solution determines the initial stages of the boundary-layer flow past an impulsively started translating and spinning rotational symmetric body of general shape. The stream function and the swirl velocity series are in terms of the local body radius $r(x)$ and the axial boundary layer edge velocity $U_e(x)$. An application of the present results requires the shape of the body and the potential flow solutions to be known.

The friction drag on the body may be written as

$$D_f = 2\pi \int_0^{l^*} r^* \tau_{wx} \cos\alpha \, \mathrm{d}x^* , \tag{4.1}$$

where l^* is the length of the body measured along the surface and α is the angle local axial tangent line makes with the symmetry axis. The moment applied to the body to maintain the rotation is

$$M = -2\pi \int_0^{l^*} r^{*2} \tau_{w\Theta} \, \mathrm{d}x^* . \tag{4.2}$$

The wall shear stresses are defined by

$$\tau_{wx} = \mu \left. \frac{\partial u^*}{\partial y^*} \right|_{y^*=0} , \qquad \tau_{w\Theta} = \mu \left. \frac{\partial w^*}{\partial y^*} \right|_{y^*=0} , \tag{4.3}$$

where μ is the viscosity of the fluid. Substitution of Eqs (4.3) and the use of the boundary layer variables reduce the friction drag and the moment to

$$D_f = 2\pi\mu \, \frac{U_0 L}{K} \int_0^l r U_e \left. \frac{\partial^2 F}{\partial n^2} \right|_{n=0} \cos\alpha \, \mathrm{d}x , \tag{4.4}$$

$$M = -2\pi\mu\omega \, \frac{U_0 L^2}{K} \int_0^l r^3 \left. \frac{\partial G}{\partial n} \right|_{n=0} \mathrm{d}x , \tag{4.5}$$

where $l = l^*/L$. Determination of the friction drag and the moment requires the local body radius and the boundary layer edge velocity to be known. Here the results are applied to an impulsively started translating and spinning sphere of radius R for which

$$L = R , \qquad l = \pi , \qquad r = \sin x , \qquad U_e = \frac{3}{2} \sin x , \qquad \cos\alpha = \sin x . \tag{4.6}$$

Friction drag and moment coefficients for a sphere are defined as

$$C_f = \frac{D_f}{2\pi\rho U_0^2 R^2} , \qquad C_M = \frac{M}{2\pi\rho U_0^2 R^3} , \tag{4.7}$$

where ρ is the fluid density. Substitution of Eqs (4.4), (4.5), (3.1), (3.2) and (4.6) into Eqs (4.7) yields

$$\sqrt{\mathrm{Re}}\, C_f = \frac{1}{\sqrt{t}}\left\{F_0''(0) + \frac{9}{20}\, t^2\Big[F_{21}''(0) - 4F_{22}''(0) + F_{23}''(0) + F_{24}''(0) - 4F_{25}''(0) + \frac{4}{9}\,\omega^2(F_{26}''(0) - 4F_{27}''(0) + F_{28}''(0))\Big] + \cdots\right\}, \tag{4.8}$$

$$\sqrt{\mathrm{Re}}\, C_M = -\frac{1}{\sqrt{t}}\left\{\frac{2}{3}\, G_0'(0) + \frac{3}{10}\, t^2\Big[G_{21}'(0) - 4G_{22}'(0) + G_{23}'(0) + G_{24}'(0) - 4G_{25}'(0) + \frac{4}{9}\,\omega^2(G_{26}'(0) - 4G_{27}'(0))\Big] + \cdots\right\}. \tag{4.9}$$

The slopes of the leading order tangential and swirl velocity functions on the surface are $F_0''(0) = 2/\sqrt{\pi}$ and $G_0'(0) = -2/\sqrt{\pi}$. The slopes of the tangential velocity functions $F_{ij}''(0)$ $(i = 1, 2;\ j = 1 - 8)$ and the swirl velocity functions $G_{ik}'(0)$ $(i = 1, 2;\ k = 1 - 7)$ are given in Tables 1 and 2 respectively. Setting $\omega = 0$ in Eq. (4.8) gives the friction drag coefficient for a translating sphere and matches the series given by Dennis and Walker [2] exactly. Temporal variations of the friction drag and moment coefficients for a translating and spinning sphere are shown in Figs 2 and 3 respectively. It may be observed that the rotation reduces the friction drag and the moment naturally increases with the spin rate. Singular behaviour near $t = 0$ is due to the impulsive start of the motion.

Separation starts first when τ_{wx} vanishes at the rear stagnation point of the sphere where $x = \pi$. The use of the boundary layer variables in Eq. (4.3) gives this condition as

$$\left.\frac{\partial^2 F}{\partial n^2}\right|_{n=0} = 0$$

and upon substitution of Eqs (3.1) and (4.6), separation time t_s may be solved from

$$F_0''(0) - \frac{3}{2}\, t_s[F_{11}''(0) + F_{12}''(0) + \frac{4}{9}\,\omega^2 F_{13}''(0)] + \frac{9}{4}\, t_s^2\Big\{F_{21}''(0) + F_{23}''(0) + F_{24}''(0) + \frac{4}{9}\,\omega^2[F_{26}''(0) + F_{28}''(0)]\Big\} = 0. \tag{4.10}$$

Table 1. Slopes of the tangential velocity functions, $F_{ij}''(0)$

i \ j	1	2	3	4	5	6	7	8
1	1.607278	0.170581	0.820061					
2	−0.248106	−0.067423	−0.032463	0.035587	−0.022623	−0.249122	−0.008566	−0.116089

Table 2. Slopes of the swirl velocity functions, $G_{ij}'(0)$

i \ j	1	2	3	4	5	6	7
1	−0.170581	−0.787217					
2	−0.080817	−0.045232	−0.292481	0.064595	0.099243	−0.188473	−0.027467

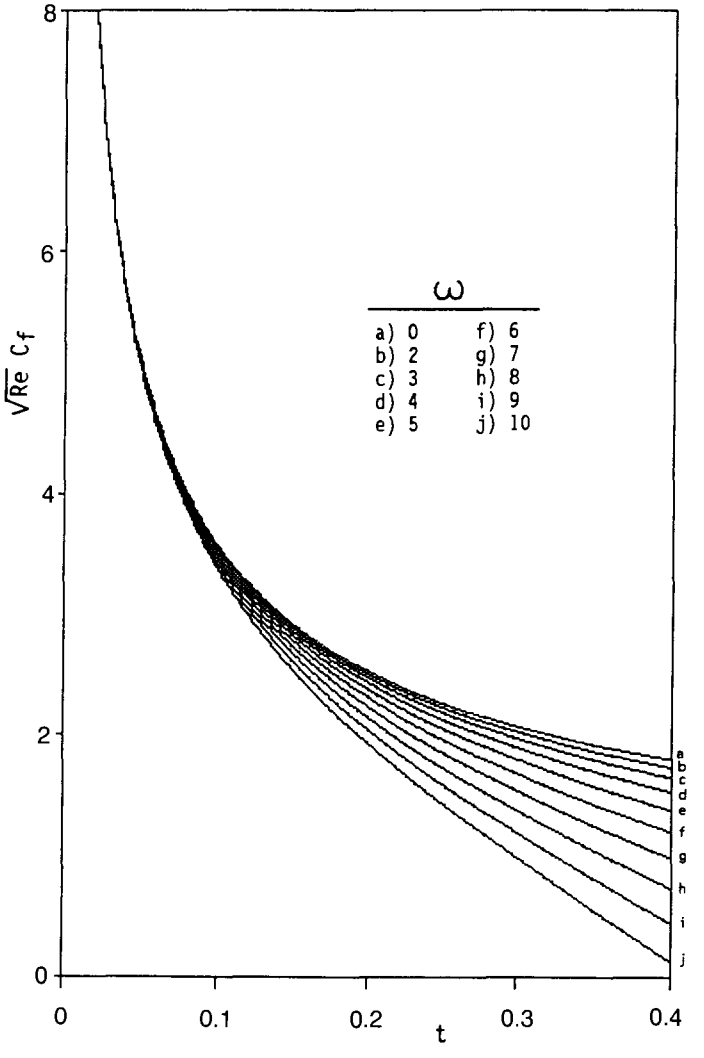

Fig. 2. Temporal variation of the friction drag coefficient for a translating and spinning sphere.

Separation times for various values of ω are given in Table 3. The results show that increasing the spin rate causes a sooner onset of separation.

The location of separation at any instant of time may be determined from

$$\left.\frac{\partial^2 F}{\partial n^2}\right|_{n=0} = 0 .$$

Similarly, with the substitution of Eqs (3.1) and (4.6), the location of separation for a translating and spinning sphere may be determined from

Table 3. Variation of the separation time with the rotation rate

ω	0	1	2	3	4	5	6	7	8	9	10
t_s	0.3915	0.3216	0.2136	0.1390	0.0939	0.0665	0.0490	0.0374	0.0294	0.0237	0.0194

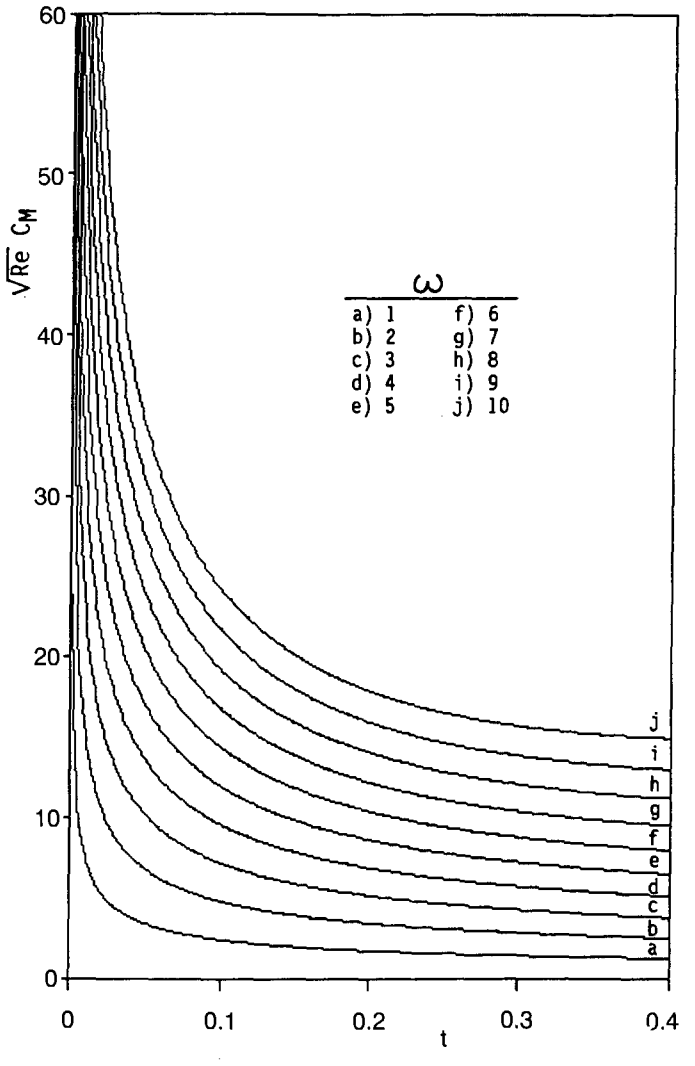

Fig. 3. Temporal variation of the moment coefficient for a translating and spinning sphere.

$$F_0''(0) + \frac{3}{2}\, t \cos x\left[F_{11}''(0) + F_{12}''(0) + \frac{4}{9}\,\omega^2 F_{13}''(0)\right] + \frac{9}{4}\, t^2\Big\{\cos^2 x[F_{21}''(0) + F_{23}''(0) + F_{24}''(0)]$$

$$- \sin^2 x[F_{22}''(0) + F_{25}''(0)] + \frac{4}{9}\,\omega^2[\cos^2 x(F_{26}''(0) + F_{28}''(0)) - \sin^2 x F_{27}''(0)]\Big\} = 0\,. \qquad (4.11)$$

Equation (4.11) is solved for x for given values of time and rotation rate. Angle of separation ϕ, measured counterclockwise from the rear stagnation point, is then obtained as $\phi = x - \pi$. Temporal variation of the angle of separation is shown in Fig. 4. The point of separation advances upstream initially very fast with a rate increasing with the spin rate. However, the advancement rate is drastically reduced with time and the separation angle increases toward its steady state value slowly. For a given time, the angle of separation is larger for a higher spin rate. This is in agreement with the results of Hoskin [7].

Development of the flow field is illustrated in Fig. 5 for $\omega = 2$. Figure 5a shows the streamlines at $t = 0.2$, shortly before separation, for this case. The next stage for which

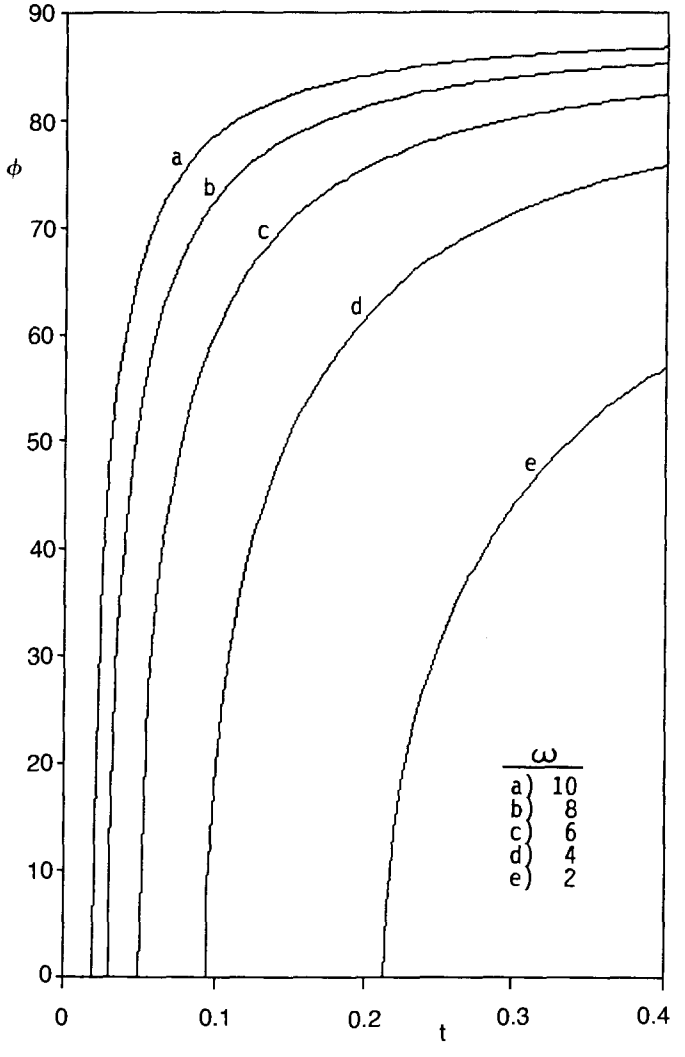

Fig. 4. Temporal variation of the separation angle for a translating and spinning sphere.

$t = 0.3$ is shown in Fig. 5b where the flow has a narrow zone of separation near the surface. Figure 5c shows the streamlines at $t = 0.4$. Separated region has grown further at this stage.

Development of the flow field for $\omega = 6$ is illustrated in Fig. 6. In this case, the rate of rotation is high enough to cause an early separation. The streamlines at $t = 0.1$ are shown in Fig. 6a. At this stage, separation is confined to a relatively narrow region. The next stage for which $t = 0.25$ is shown in Fig. 6b where the separated region has grown considerably. The separated region continues to grow intensively and the flow field at $t = 0.4$ is shown in Fig. 6c.

The time series solution obtained in the present paper for an impulsively started translating and spinning rotational symmetric body of general shape is limited to the early stages of the boundary layer flow. The time series were truncated after the terms of $O(t^2)$ and the neglected terms are of $O(t^3)$ and $O(t^3\omega^2)$. The general results applied to an impulsively started translating and spinning sphere were pushed up to $t = 0.4$. The functions in the streamwise and circumferential velocity series gradually decrease in magnitude as the

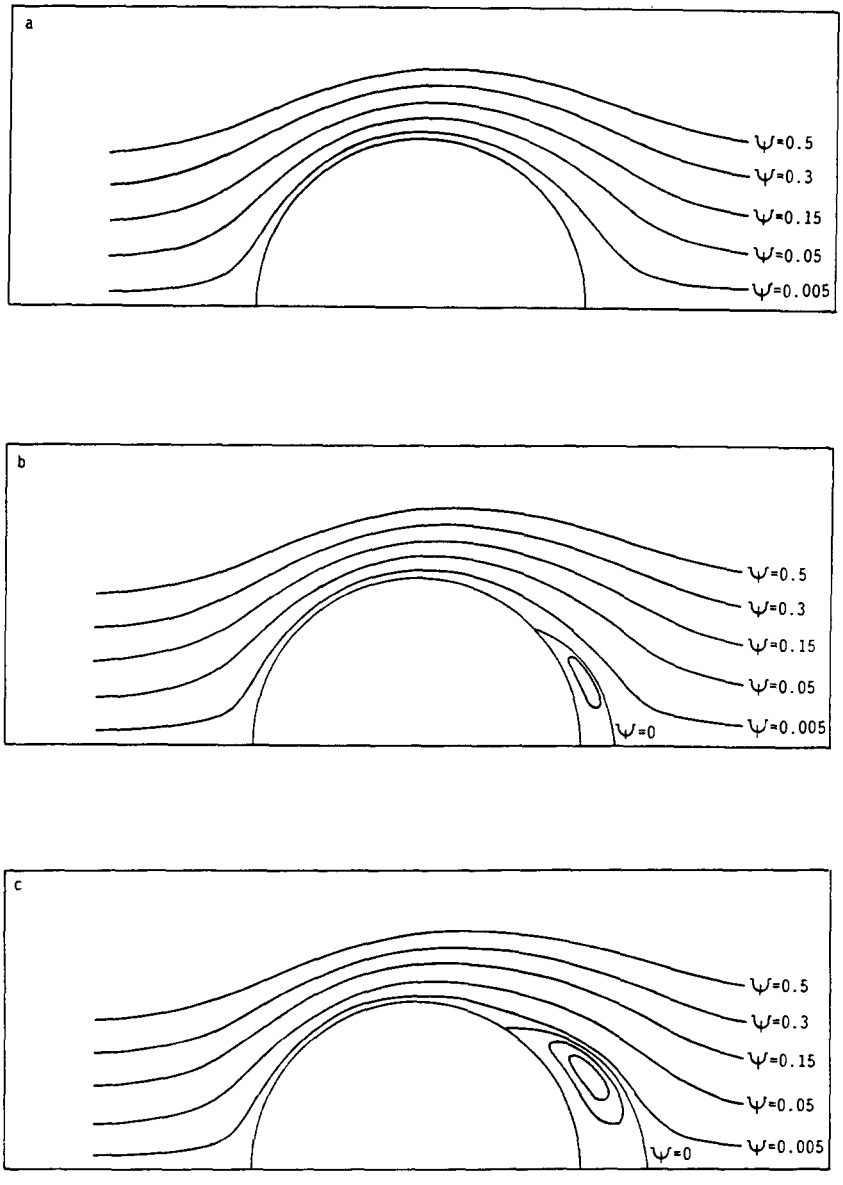

Fig. 5. Temporal development of the flow field for $\omega = 2$ at (a) $t = 0.2$, (b) $t = 0.3$ (enclosed streamline is -0.0002) and (c) $t = 0.4$ (enclosed streamlines from the center are -0.004 and -0.002).

order of the functions increases. The functions related to t^2 and $t^2\omega^2$ are $O(10^{-1})$ and $O(10^{-2})$ at most. Thus the solutions at $t = 0.4$ for $\omega \leq 10$ are at worst one digit accurate and the accuracy improves to two digits for small ω. For example, in the case of a translating sphere for which $\omega = 0$, the separation time was obtained with two digit accuracy as $t_s = 0.3915$. Accuracy of the solutions naturally increases as t decreases. The solutions are three digit accurate for $t \leq 0.2$ and two digit accurate for $t \leq 0.4$ provided $\omega = O(1)$. Numerical integration of the boundary layer equations is necessary to extend the solutions to larger values of time. A particular body shape may require a different numerical analysis and treatment.

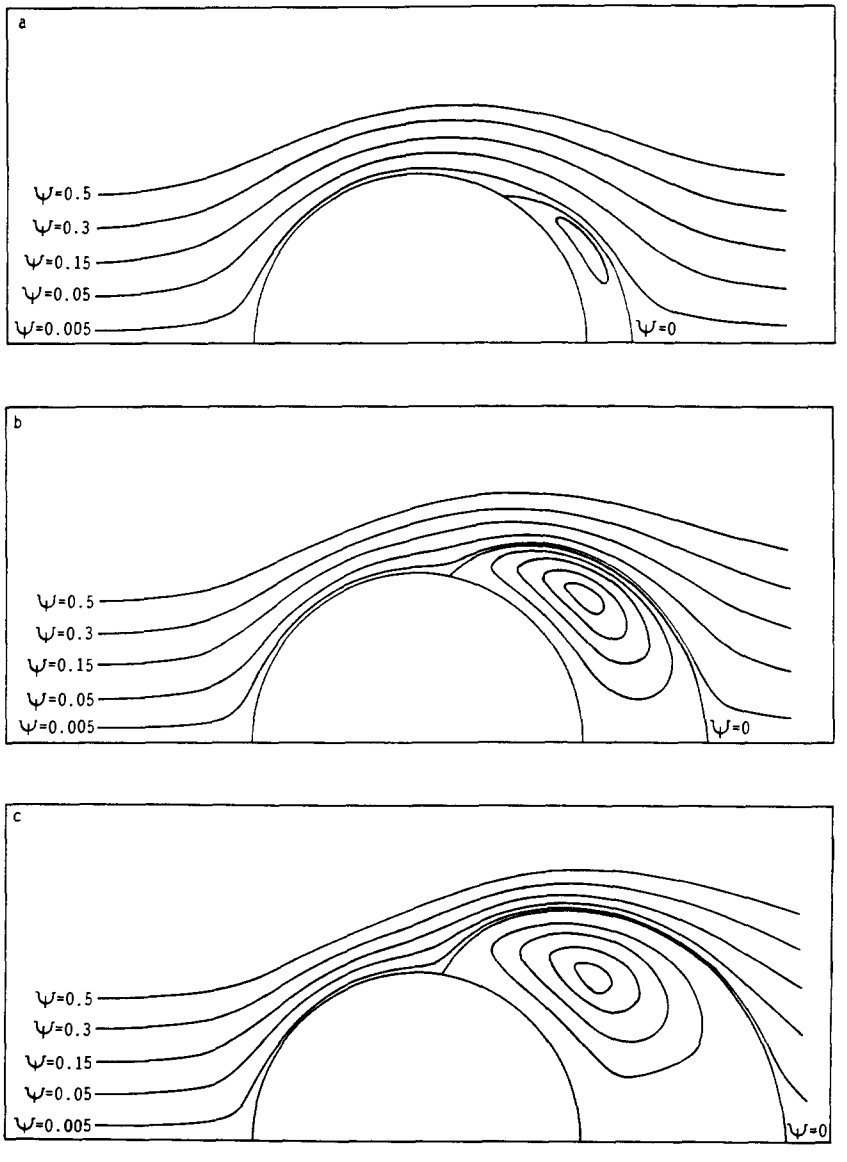

Fig. 6. Temporal development of the flow field for $\omega = 6$ at (a) $t = 0.1$ (enclosed streamline is -0.002), (b) $t = 0.25$ (enclosed streamlines from the center are -0.1, -0.08, -0.05 and -0.02) and (c) $t = 0.4$ (enclosed streamlines from the center are -0.33, -0.28, -0.2 and -0.1).

References

1. E. Boltze, Grenzschichten an Rotationskörpern in Flüssigkeiten mit Kleiner Reibung. Thesis, Göttingen (1908).
2. S.R.D. Dennis and J.D.A. Walker, The initial flow past an impulsively started sphere at high Reynolds numbers. *Journal of Engineering Mathematics* 5 (1971) 263–278.
3. S.R.D. Dennis and J.D.A. Walker, Numerical solutions for time-dependent flow past an impulsively started sphere. *The Physics of Fluids* 15 (1972) 517–525.
4. C.R. Illingworth, The laminar boundary layer of a rotating body of revolution. *Phil. Mag.* 44 (1953) 351–389.
5. S.T. Chu and A.N. Tifford, The compressible laminar boundary layer on a rotating body of revolution. *JAS* 21 (1954) 345–346.

6. H. Schlichting, Die Laminare Strömung um Einen Axial Angeströmten Rotierenden Drehkörper. *Ing. Arch.* 21 (1953) 227–244.
7. N.E. Hoskin, The laminar boundary layer on a rotating sphere. In: W. Tollmien and H. Görtler (eds), *Fifty Years of Boundary Layer Research*. Braunschweig (1955) pp. 127–131.
8. L. Howarth, The boundary layer in three-dimensional flow, Part I. *Phil. Mag.* 42 (1951) 239–243.
9. O. Sawatzki, Strömungsfeld um Eine Rotierende Kugel. *Acta Mech.* 9 (1970) 159–214.
10. P. Dumarque, G. Laghoviter and M. Daguenet, Determination des lignes de courant parietales sur un corps de revolution tournant autour de son axe dans un fluide au repos. *ZAMP* 26 (1975) 325–336.
11. S. Lutander and A. Rydberg, Experimentelle Untersuchungen über den Luftwiderstand bei Eine um Eine mit der Windrichtung Parallel Achse Rotierenden Kugel. *Phys. Z.* 36 (1935) 552–558.
12. W. Mangler, Ber. Aerodyn. Versuchsanst. Goett. Rep. 45/A/17 (1945).
13. M.C. Ece, T.L. Doligalski and J.D.A. Walker, The boundary layer on an impulsively started rotating and translating cylinder. *Physics of Fluids* 27 (1984) 1077–1089.